

Peng Cui^{1,2},
Yuan Xue^{1,*}

Simulation of the Colour Appearance of Weft-Knitted Fabric by Extracting and Mapping Colour Textures of Coloured Spun Yarn

DOI: 10.5604/01.3001.0014.3795

¹ Jiangnan University,
Key Laboratory of Eco-Textiles,
Wuxi, 214021,
Jiangsu, P.R. China,
* e-mail: fzxueyuan@qq.com

² Yuyue Home Textile Co Ltd,
Binzhou, Shandong, P.R. China

Abstract

In the present work, we propose a framework of simulating the colour appearance for weft-knitted fabric. A self-developed image capturing apparatus was used to record an image of coloured spun yarn. Pierce's loop model was used for the colour mapping of weft-knitted fabrics. According to the algebraic-geometric relation of Pierce's loop model, the colour information of the coloured spun yarn is mapped onto the loop. We found there exist „black spots” on the simulated needle loop and sinker loop due to the mismatch between the pixels of the yarn and the arc of the loop, which can be resolved by the interpolation fitting procedure. Moreover, changing the loop length offers a way to control the pattern of weft-knitted fabric. Finally, the brightness values at different positions of the loop were calculated in HSV color space to generate virtually realistic textures of the simulated weft-knitted fabric.

Key words: weft-knitted fabric, Pierce's loop model, colour mapping, coloured spun yarn.

■ Introduction

In the textile industry, varying fabric structures and dyeing [1, 2] raise economic interest in textile products. Knitted fabrics have a variety of structures, including stockinette, garter and rib [3], and thus can be combined with coloured spun yarns to form different appearances and patterns. The texture features of yarn are critical for the appearance of knitted fabrics [4]. In particular, coloured spun yarn brings abundant colour patterns to knitted fabrics by manipulating the total length of the yarn and segmental arrangement [5, 6]. Therefore, coloured spun yarn is especially promising for the dressing market.

The extraction of texture information from colored spun yarn is essential for simulating the appearance of fabric, which can be done by recording yarn images via an electronic device, followed by the extraction of textural properties, that is, information on the evenness, colour and diameter of the coloured spun yarn, based on the segmentation algorithm. Then, the texture information of the coloured spun yarn extracted is mapped

onto a two-dimensional computer-based geometrical model of the coloured spun yarn, which is subsequently used to simulate the appearance of fabrics.

Simulating the appearance of fabrics is one of the open challenges in computer graphics due to the very small scale of fibres and complicated light-matter interaction. There are two approaches to generating the appearance of fabric, i.e., the forward generative solution and reverse engineering solution [7]. In the former case, the structure of the fabric is modelled at the scale of a single fibre or at the yarn level; however, a large number of input parameters are required to simulate a fabric, which is challenging to put into practical use due to the high computational cost. In the latter case, the fabric geometry or the appearance of the fabric is captured using electronic devices, such as simple photographic cameras [8, 9], gonireflectometers [10, 11], camera forests [12], and volume scans [13, 14], among which the volume scans method is able to achieve plausible results since it can reach micron resolution using a CT scanner, followed by utilization of orientation kernels to generate a realistic heterogeneous structure of the fabric. The reverse engineering approach is more reliable in reproducing the appearance of fabric than the forward generative approach since the forward generative approach typically lacks the specification of fibre types, fibre structures, the dye property, and manufacturing processes for the fabric. However, the reverse en-

gineering approach relies on estimating the similarity between a simulated image and a photograph, which largely depends on the material-handling process, such as the angular distribution of samples [15]. Thus, the reverse engineering approach is not effective in simulating the appearance of colour blended fabric since it cannot catch the important colour features at the yarn or fibre level [16].

In the present work, we establish a framework for simulating the colour appearance of weft-knitted fabric, which is easier to make and more common in comparison with warp knitted fabric. A self-developed image capturing apparatus was used to record an image of coloured spun yarn. Subsequently, the digital images captured were processed to produce spatially corresponding pixels to reconstruct digital images of the object, including image graying, filtering, morphology processing and image segmentation. Pierce's elliptical model [17, 18], which is composed of three parts: a sinker loop, legs of the loop, and a needle loop, is used to represent the loop geometry of weft-knitted fabric. By establishing a mathematical description of Pierce's elliptical model, the color information of the yarn image can be mapped onto the loop by establishing a one-to-one correspondence between the pixels of the coloured spun yarn and the loop. Subsequently, the light intensities at different positions of the loop, which is adjusted to recover the surface reflectance of textiles.

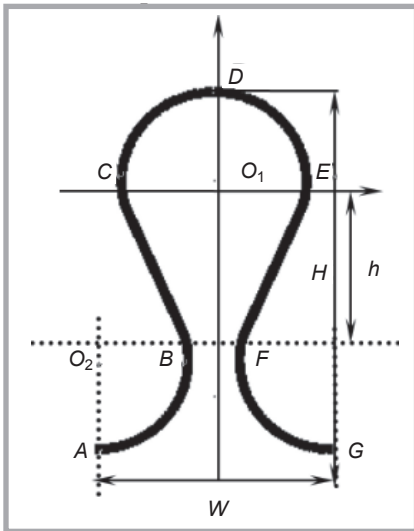


Figure 1. Pierce's loop model.

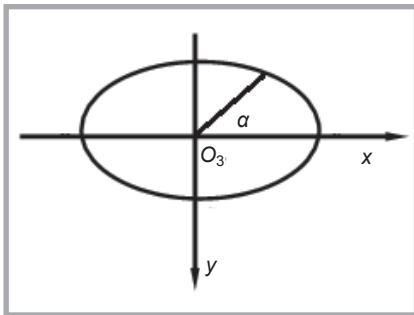


Figure 2. Schematic diagram depicting the elliptic coordinate system.

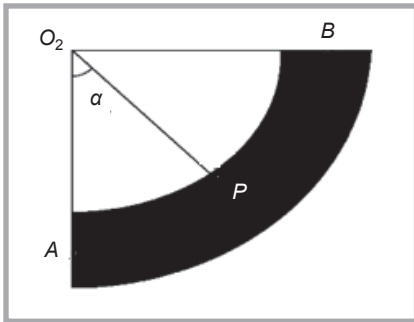


Figure 3. AB area of the sinker loop.

Theoretical model

Extracting the texture feature of yarn using the k-means segmentation algorithm

The k-means algorithm is an iterative algorithm that tries to partition data and seeks an optimal solution to the clustering criterion function of each partitioned cluster, thereby maximising intra-cluster similarity and the inter-cluster difference between the partitioned data clusters [19]. The recorded yarn image is partitioned into several clusters, and the initial centroid of each cluster should be

preset when using the k-means clustering segmentation algorithm. Therefore, selecting the number of clusters and initial cluster centers is crucial for the correctness of clustering. The number of clusters selected should be in line with the best partitioning of samples. Otherwise, a different number of clusters may result in totally different clustering results and increase the processing time [20]. Therefore, data partitioning is required for each iteration of the algorithm to ensure the data are as close to each cluster as possible. When all data are included in its cluster, one round of the iterative process is completed, and new centroids will replace the old ones.

A mathematical description of the loop model of weft-knitted fabric

Pierce's model is a universal loop model [18, 20, 21], which assumes that the yarns are fully relaxed in the knitted fabric, and thus can be represented by a generalised geometric model. As shown in Figure 1, the loop is composed of five parts: arc AB, line segment BC, arc CDE, line segment EF and arc FG. The left and right sides of the loop are symmetric about the y-axis. Arc AB and arc FG refer to the left and right sinker loops respectively; arc CDE is the needle loop, and straight lines BC and EF represent the left and right legs of the loop, respectively. The needle loop and sinker loop are treated as ellipses, and a & b are the half-width and half-height of the ellipse, respectively.

A rectangular coordinate system with the O_1 point as the origin is established, where X_0 and Y_0 are the coordinates of the origin, respectively. Then, the x and y coordinates of each point in Figure 1 can be obtained as follows:

$$\begin{cases} A(x, y) = \left(X_0 - \frac{W}{2}, Y_0 + h + b\right) \\ B(x, y) = \left(X_0 - \frac{W}{2} - a, Y_0 + h\right) \\ C(x, y) = (X_0 - a, Y_0) \\ D(x, y) = (X_0, Y_0 - b) \\ E(x, y) = (X_0 + a, Y_0) \\ F(x, y) = \left(X_0 + \frac{W}{2} - a, Y_0 + h\right) \\ G(x, y) = \left(X_0 + \frac{W}{2}, Y_0 + h + b\right) \end{cases} \quad (1)$$

where, H is the height of the loop, $H = 5a$; W is the distance between loops, $W = 3a$, and h is the longitudinal spacing between the needle loop and sinker loop, $h = H - 2b$.

Colour mapping from the coloured spun yarn to the loop

The slopes of the line BC and EF are assumed to be K_1 and K_2 , the mathematical expression of which can be obtained according to the coordinates of points B, C, E, and F.

$$\begin{cases} K_1 = \frac{Y_0}{X_0 - \left(\frac{W}{2} - a\right) - (X_0 - a)} \\ K_2 = \frac{-Y_0 - h}{(X_0 + a) - \left(X_0 + \left(\frac{W}{2} - a\right)\right)} \end{cases} \quad (2)$$

The coordinates of the arbitrary pixels on the line segment BC and EF can be obtained based on K_1 and K_2 , as shown in Equations (3) and (4), respectively

$$\begin{cases} y = i_{BC} \\ x = \frac{i_{BC} - (Y_0 + h)}{K_1} + X_0 - \left(\frac{W}{2} - a\right) \end{cases} \quad (3)$$

$$\begin{cases} y = i_{EF} \\ x = \frac{(i_{EF} - Y_0)}{K_2} + X_0 + a \end{cases} \quad (4)$$

Where, i_{BC} and i_{EF} are the y coordinates of arbitrary pixels from line BC and EF, respectively. Then, the colour information of the spun yarn is mapped onto the legs of the loop according to the following Equation (5).

$$L[Q_x, Q_y, z] = Y[R_x, R_y, z] \quad (5)$$

Where, the left side of the equation corresponds to the pixel-matrix element of the legs of the loop, while the right side of the equation corresponds to the pixel-matrix element of the coloured spun yarn. Q_x and Q_y are the x and y coordinates of an arbitrary pixel in the legs of the loop, respectively; z marks the R, G, and B colour components, and R_x and R_y represent the coordinates of corresponding pixels in the coloured spun yarn.

To complete the colour mapping of the coloured spun yarn onto the arc, we establish a mathematical description of the arc based on the elliptical coordinate system. Assuming O_3 is the origin, α represents the angle originating at O_3 , which varies from 0 to 2π , as shown in Figure 2.

Based on the algebraic relationship in Equation (1), when $3\pi/2 < \alpha < 2\pi$, the curve equation of the left sinker loop AB is obtained, as shown in Equation (6); when $-\pi < \alpha < 0$, the curve equation of the needle loop CDE is obtained, as shown

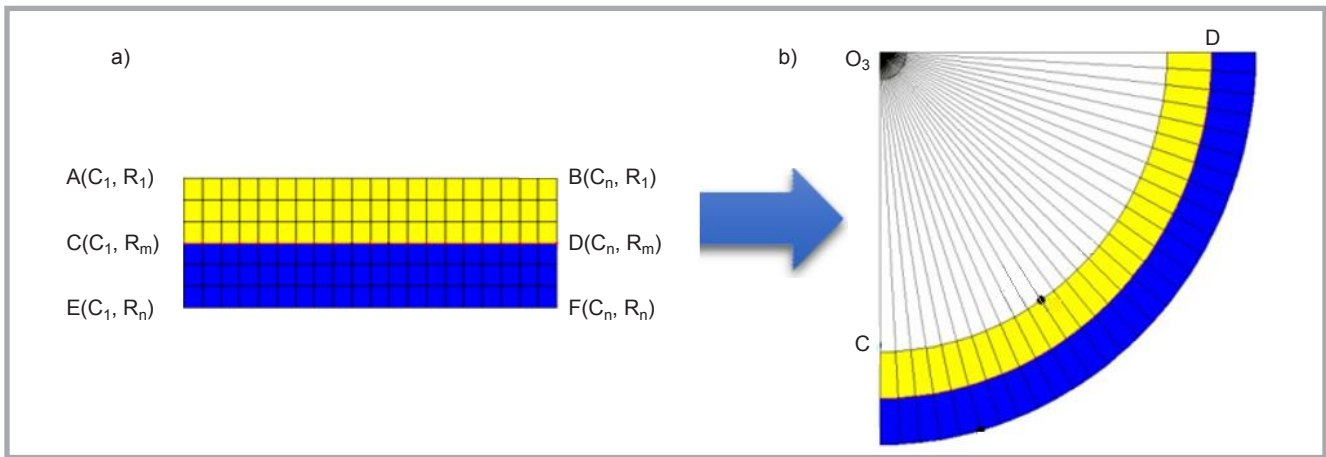


Figure 4. a) Schematic diagram illustrating a pixel model of the yarn; b) a schematic diagram illustrating a pixel model of the arc.

in Equation (7); and when $\pi < \alpha < 3\pi/2$, the curve equation of the right sinker loop FG is obtained, as shown in Equation (8).

$$\begin{cases} y = Y_0 - b\sin\alpha + h \\ x = X_0 + a\cos\alpha - \frac{W}{2} \end{cases} \quad (6)$$

$$\begin{cases} y = Y_0 - b\sin\alpha + h \\ x = X_0 + a\cos\alpha + \frac{W}{2} \end{cases} \quad (7)$$

$$\begin{cases} y = Y_0 - b\sin\alpha \\ x = X_0 + a\cos\alpha \end{cases} \quad (8)$$

As shown in Figure 3, P represents the arbitrary pixel in the arc AB . According to Equation (4), the x and y coordinates of the origin O_2 are $(X_0 - W)/2$ and $Y_0 + h$, respectively. K_3 , the slope of O_2P , can be obtained based on the coordinates of O_2 and P , the mathematical expression of which is given in Equation (9).

$$\begin{cases} K_3 = \frac{-b\sin\alpha}{X_0 + a\cos\alpha - \frac{W}{2} - (X_0 - \frac{W}{2})} \\ y_{O_2P} = K_3(x - (X_0 - W)) + (Y_0 + h) \end{cases} \quad (9)$$

Where, y_{O_2P} is the ordinate of point P . Assuming x_{O_2P} is the abscissa of point P , one can establish a one-to-one correspondence between the pixels of the arc and yarn. Subsequently, the pixel of the yarn is mapped onto the arc, according to Equation (5).

Figure 4 illustrates the process of colour mapping from the yarn to the arc. Figure 4.a is a schematic diagram depicting the pixel-matrix model of the yarn, where CD is the centerline of the yarn, and (C_i, R_j) is the index pair associated with the meshing element. Figure 4.b

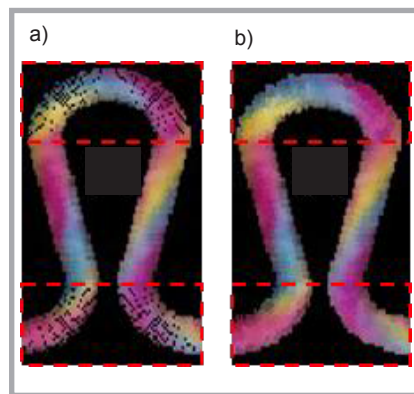


Figure 5. a) Simulated loops before performing the interpolation fitting procedure and b) after performing the interpolation fitting procedure.

is a schematic diagram depicting a pixel model of the arc with a radius of $\pi/2$, where O_3 is the circle centre. The centerline of the sinker loop is equally divided into p sectors with a radius of $\Delta\alpha$, as shown in Equation (10).

$$\Delta\alpha = \frac{\frac{\pi}{\alpha} \times r \times \pi}{2} \quad (10)$$

The pixel densities on the centerlines of the yarn and arc are the same; therefore, we can establish a one-to-one correspondence between the pixels of the yarn and arc; however, the pixel density in the yellow region of the sinker loop is less than that of the yarn, while the pixel density in the blue region of the sinker loop is greater than that of the yarn. Therefore, when the pixel information in the yellow and blue regions of the yarn is mapped onto the arc, the positions of the pixels are misaligned with each other. As shown in Figure 5.a, the black spots on the arc are caused by the mismatch of the pixel information between the arc and the yarn.

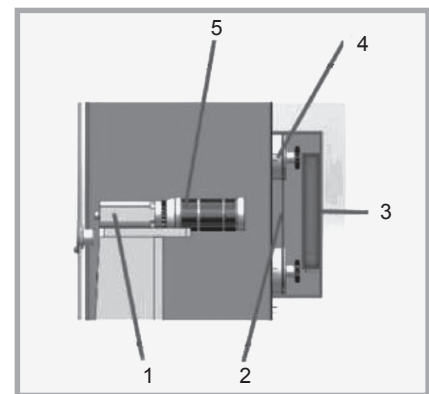


Figure 6. Yarn image acquisition device; 1 – CCD area image sensor, 2 – yarn, 3 – light source, 4 – yarn guide device, 5 – camera lens.

As such, the interpolation fitting procedure [23] is carried out to ensure the continuity of the pixels of the arc, as shown in Figure 5.b.

Using the same principle, colour mapping of arcs CDE and FG is performed to yield the simulated loop of the weft-knitted fabric.

Methodology

In the present work, we used an image capturing apparatus developed by the Research Institute of Textile Technology at Jiangnan university to record the yarn image, shown in Figure 6. Colour images were recorded by a single high-resolution colour charge-coupled device (CCD) sensor and saved in BMP, TIF or JPG image formats. The output image size is 56×473 pixels, and the physical size of the image is calibrated to 1 cm. This experimental setup can also be adapted to measure the photometric properties of selected retroreflective materials on

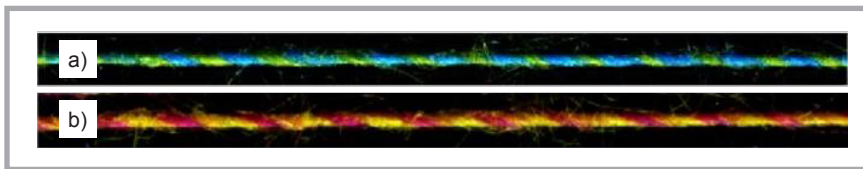


Figure 7. Recorded images of two-coloured spun yarn with different combinations of colours and blending ratios using self-developed image capturing apparatus: a) yellow:blue = 3:7, b) red:yellow = 7:3.

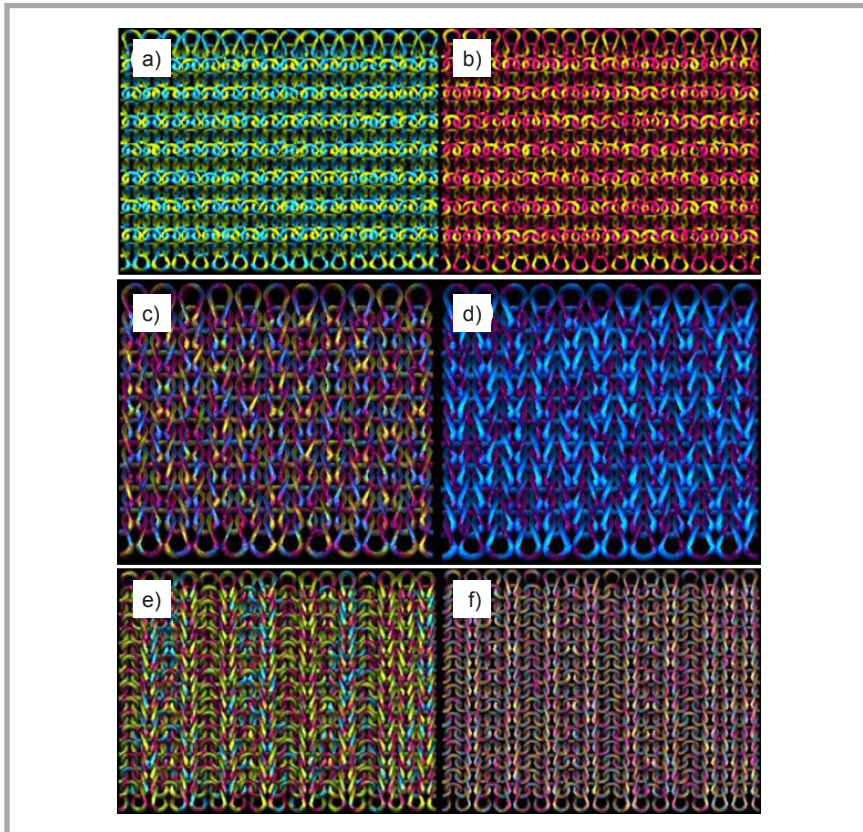


Figure 8. Simulated weft-knitted fabrics using extracted images of colored spun yarns: a) yellow:blue = 3:7, b) red:yellow = 7:3, c) red:yellow:blue = 4:4:2, d) red:blue = 5:5, e) red:yellow:blue = 3:3:4, f) red:yellow:blue = 4:4:2.

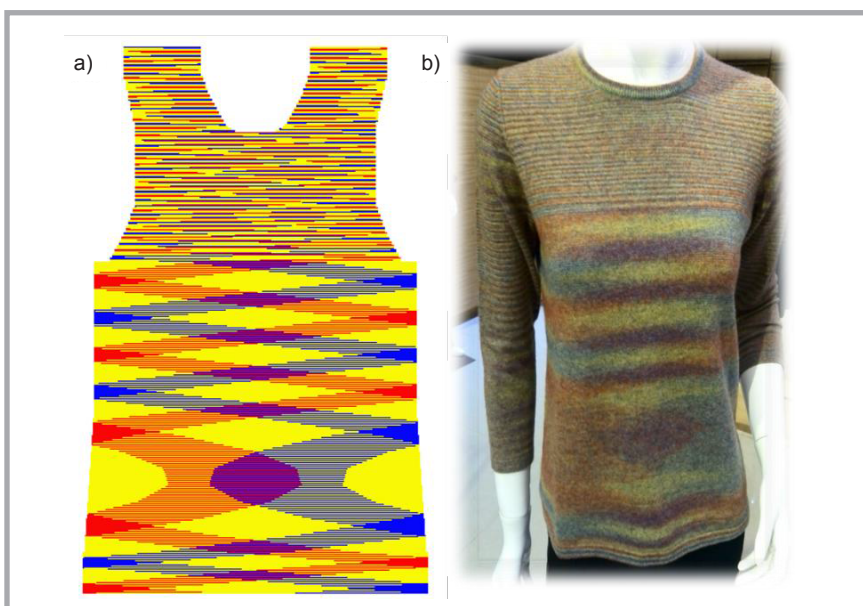


Figure 9. a) Simulated knit fabric; b) photograph of knit fabric.

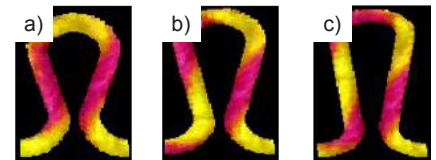


Figure 10. Loop shapes under different l values: a) $l = 150$; b) $l = 250$; c) $l = 300$.

a textile base or polymer base, as demonstrated in Pościk et al.'s work [24].

The weighted average method is used to convert the colour image into a grayscale one [25, 26]. Then, median filtering is performed to eliminate isolated noise pixels [27]. Moreover, the opening operation of mathematical morphology is used to remove sharp objects in the image [28, 29]. Finally, the k-means segmentation algorithm is performed to extract texture features of the coloured spun yarn.

Results and discussion

Figure 7 shows images of the two-coloured spun yarn recorded using the self-developed image capturing apparatus. **Figure 8** shows the simulated appearance of weft-knitted fabrics made of two-coloured spun yarns and three-coloured spun yarns, respectively. **Figure 9** shows a comparison of the images of the simulated and actual knit fabrics. It is found that the main colour textures of the coloured spun yarn are well preserved in the simulated knit fabric, indicating adequate validity of our proposed colour mapping framework.

Effect of loop length

The loop length not only determines the mechanical properties of weft-knitted fabric but also influences the color pattern of colored spun yarn, which consists of a succession of segments of different colours. Therefore, the loop length is critical for the simulated appearance of weft-knitted fabric.

According to **Figure 1**, the loop structure consists of arc AB , line segment BC , arc CD , arc DE , line segment EF , and arc FG . The size of each component is determined by the geometric parameters of the loop model, such as H , W , h , a , and b . Therefore, the most basic parameters of the loop model, i.e., the half-width a and half-height b of the ellipse, can be tuned by adjusting the value of l , which accordingly gives different sizes and shapes of the loop, as shown in **Figure 10**.

Therefore, the colour pattern of colour blended knitted fabric can be modified on the computer screen by tuning the yarn length, which benefits the computer-aided design of weft-knitted fabrics.

Tuning the brightness of the knitted fabric

Brightness is varied at different parts of the loop surface due to the contact regions between loops. Therefore, local illumination is applied to different positions of the loop to display virtually realistic textures of the simulated weft-knitted fabric. Here, we adopt a structural approach [30] that predicts the brightness variation characteristics based on the bending curves at the surface of yarns.

Figure 11 shows the schematics of three common structures of weft-knitted fabric, i.e., plain-knitted fabric, rib-knitted fabric and purl-knitted fabric. It can be seen that the arc is always covered by the legs of the loop on the front side of the plain-knitted fabric, while the legs of the loop are always covered by the arc on the opposite side. It is assumed that the height of the loop is K and that the longitudinal distance from each pixel N to the top of the loop is $|N_y - K_y|$. The brightness values at different positions on the loop can be obtained according to the brightness variation curves of the textures at the surface of the loop [30].

Where, $L_1, L_2, L_3,$ and L_4 are different brightness values of the loops; L_0 represents the initial brightness of the loop; L_{min} and L_{max} are the minimum and maximum brightness values, respectively; H is the overall height of the loop; N_y refers to the y -axis coordinate of each point of the loop, and L_r is an adjustable parameter. The brightness values expressed in the HSV colour space can show the changes in hue, saturation, and lightness, which is more suitable for the visual characteristics of humans than the RGB colour space. During the simulation, the $r, g,$ and b components in the RGB color space are converted to $h, s,$ and v components in the HSV color space. The brightness value is calculated according to **Equations (11)-(14)** and then assigned to colour component v . Next, the brightness values in the HSV color space are converted back into the RGB color space to display the variation in brightness at different parts of the loop, as shown in **Figure 12.a-12.d**. The variation characteristics of the brightness of

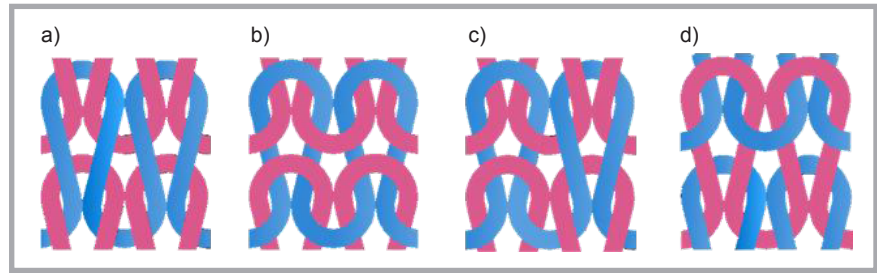


Figure 11. Schematic diagram of structures of: a) front side of plain-knitted fabric, b) back side of plain-knitted fabric, c) rib-knitted fabric and d) purl-knitted fabric.

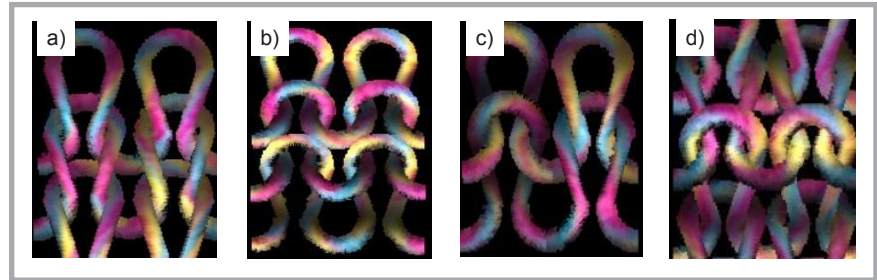


Figure 12. Simulated weft-knitted fabrics with the variation in brightness at different parts of the loop: a) front side of plain-knitted fabric, b) back side of plain-knitted fabric, c) rib-knitted fabric, d) purl-knitted fabric.

the loop are consistent with Lu et al.'s result [30], indicating the validity of our simulation.

Conclusions

In this work, we propose a theoretical framework for reproducing the colour appearance of weft-knitted fabrics made of coloured spun yarn. An image of the coloured spun yarn was recorded using a self-developed image capturing apparatus, followed by a series of processing steps to remove the image noise pixels, which was subsequently used for colour mapping. A one-to-one correspondence is established between Pierce's loop model and the colored spun yarn image, in which the pixel information of

the spun yarn is mapped onto the corresponding positions of the loop. However, it is found that there exists a certain mismatch between the pixel information of the arc of the loop and the spun yarn, which needs to be dealt with by means of the interpolation fitting procedure to ensure the continuity of colour mapping. Moreover, changing the length of the loop changes the pattern as well as the shape of coloured spun yarn, which accordingly alters the simulated appearance of weft-knitted fabric made of coloured spun yarn. Furthermore, the brightness values at different positions of the loop are calculated in HSV color space to make the colour texture of weft-knitted fabric appear realistic. □

$$L_1 = L_0 + \frac{L_{max} - L_0}{2} \left(1 - \cos \left(\frac{2\pi(N_y - K_y)}{H} \right) \right) \quad (11)$$

$$L_2 = L_0 + \frac{L_0 - L_{min}}{2} \left(\cos \left(\frac{2\pi(N_y - K_y)}{H} \right) - 1 \right) \quad (12)$$

$$L_3 = L_0 + (L_{max} - L_0 - L_r) \sin \frac{2\pi(N_y - K_y)}{H} + 2L_r \sin \left(\frac{4\pi(N_y - K_y)}{H} + \pi \right) \quad (13)$$

$$L_4 = L_0 + (L_{max} - L_0 - L_r) \sin \left(\frac{2\pi(N_y - K_y)}{H} + \pi \right) + 2L_r \sin \left(\frac{4\pi(N_y - K_y)}{H} \right) \quad (14)$$

Equations (11), (12), (13) and (14).

Acknowledgements

This work is supported by "Fundamental Research Funds for the Central Universities" under Grant "JUSRP12029" and "JUSRP 52007A".

References

1. Samanta AK, Konar A. Dyeing of textiles with natural dyes. *Natural dyes*. 2011; 3:30-56.
2. Weiser J, Raulfs FW, Siemensmeyer K. Digital Textile Printing, NIP & Digital Fabrication Conference. *Society for Imaging Science and Technology* 2000; 529-532.
3. Cho S, Cho G, Kim C. Fabric Sound Depends on Fiber and Stitch Types in Weft Knitted Fabrics. *Textile Research Journal* 2009; 79(8):761-767.
4. Kliman HL, Pike RH. Method of Simulating by Computer the Appearance Properties of a Fabric, Google Patents, 1991.
5. Yang RH, Han RY, Lu YZ, Xue Y, Gao WD. Color Matching of Fiber Blends: Stearns-Noechel Model of Digital Rotor Spun Yarn. *Color Research & Application* 2018; 43(3):415-422.
6. Yang R, Xu Y, Xie C, Wang H. Kubelka-Munk Double Constant Theory of Digital Rotor Spun Color Blended Yarn. *Dyes and Pigments* 2019; 165: 151-156.
7. Bézivin J, Barbero M, Jouault F. On the Applicability Scope of Model Driven Engineering, Fourth International Workshop on Model-Based Methodologies for Pervasive and Embedded Software (MOMPES'07). *IEEE* 2007; p. 3-7.
8. Schröder K, Zinke A, Klein R. Image-Based Reverse Engineering and Visual Prototyping of Woven Cloth. *IEEE Transactions on Visualization and Computer Graphics* 2014; 21(2): 188-200.
9. Guarnera GC, Hall P, Chesnais A, Glen-cross M. Woven Fabric Model Creation From a Single Image. *ACM Transactions on Graphics (TOG)* 2017; 36(5): 165.
10. Matusik W. A Data-Driven Reflectance Model, Massachusetts Institute of Technology, 2003.
11. Dupuy J, Jakob W. An Adaptive Parameterization for Efficient Material Acquisition and Rendering, SIGGRAPH Asia 2018 Technical Papers, *ACM*, 2018; p. 274.
12. Dana KJ, Van Ginneken B, Nayar SK, Koenderink JJ. Reflectance and Texture of Real-World Surfaces. *ACM Transactions on Graphics (TOG)*. 1999; 18(1): 1-34.
13. Zhao S, Jakob W, Marschner S, Bala K. Building Volumetric Appearance Models of Fabric Using Micro CT Imaging. *ACM Transactions on Graphics (TOG)*. *ACM*, 2011; p. 44.
14. Khungurn P, Schroeder D, Zhao S, Bala K, Marschner S. Matching Real Fabrics with Micro-Appearance Models. *ACM Trans. Graph.* 2015; 35(1):1-1:26.
15. Jarabo A, Wu H, Dorsey J, Rushmeier H, Gutierrez D. Effects of Approximate Filtering on the Appearance of Bidirectional Texture Functions. *IEEE Transactions on Visualization and Computer Graphics* 2014; 20(6): 880-892.
16. Castillo C, López-Moreno J, Aliaga C. Recent Advances in Fabric Appearance Reproduction. *Computers & Graphics* 2019; 84:103-121.
17. Stump D, Fraser W. A Simplified Model of Fabric Drape Based on Ring Theory. *Textile Research Journal* 1996; 66(8): 506-514.
18. Szablewski P. Estimating Engineering Constants of Woven Textile Composite Using Geometric Model. *The Journal of the Textile Institute* 2014; 105(12): 1251-1258.
19. Jain AK. Data Clustering: 50 Years Beyond K-Means. *Pattern Recognition Letters*. 2010; 31(8): 651-666.
20. Huang LK, Wang MJJ. Image Thresholding by Minimizing the Measures of Fuzziness. *Pattern Recognition* 1995; 28(1): 41-51.
21. Dolatabadi MK, Kovař R. Geometry of Plain Weave Fabric Under Shear Deformation. Part II: 3D Model of Plain Weave Fabric before Deformation. *The Journal of the Textile Institute* 2009; 100(5): 381-386.
22. Tarfaoui M, Akesbi S. Numerical Study of the Mechanical Behaviour of Textile Structures. *International Journal of Clothing Science and Technology* 2001; 13(3/4): 166-175.
23. Zhang Z, Li BY, Liu XQ, Wang FM, Wu ZJ. Research on Texture Mapping in Weft-Knitted Fabric Simulation. *Journal of Donghua University(Natural Science)* 2011; 37(6): 745-749.
24. Pościk A, Szkudlarek J, Owczarek G. Photometric Properties of Retroreflective Materials in Dependence on their Structure and Angle of Illumination. *FIBRES & TEXTILES in Eastern Europe* 2019; 27, 3(135): 58-64. DOI: 10.5604/01.3001.0013.0743.
25. Zhongxiang H, Lei Z, Jiaxu T, Xuehong M, Xiaojun S. Evaluation of Three-Dimensional Surface Roughness Parameters Based on Digital Image Processing. *The International Journal of Advanced Manufacturing Technology* 2009; 40(3-4): 342-348.
26. Tang J, Miao R, Zhang Z, He D, Liu L. Decision Support of Farmland Intelligent Image Processing Based on Multi-Inference Trees. *Computers and Electronics in Agriculture* 2015; 117: 49-56.
27. Chen T, Ma KK, Chen LH. Tri-State Median Filter for Image Denoising. *IEEE Transactions on Image Processing* 1999; 8(12): 1834-1838.
28. Qian ZY, Hua GW, Cheng CZ, Tian TJ, Yun LL. Medical Images Edge Detection Based on Mathematical Morphology. 2005 IEEE Engineering in Medicine and Biology 27th Annual Conference. *IEEE* 2006; p. 6492-6495.
29. Chen T, Wu Q, Rahmani-Torkaman R, Hughes J. A Pseudo Top-Hat Mathematical Morphological Approach to Edge Detection in Dark Regions. *Pattern Recognition* 2002; 35(1): 199-210.
30. Lu ZW, Jiang GM. Rapid Simulation and Computer Implementation of Flat Knitting Loops Based on Yarn Texture. *Journal of Textile Research* 2016; 37(2): 119-124.

Received 7.10.2019 Reviewed 24.04.2020

